A study of using cosmic ray muon radiography to detect CO_2 leakage from a primary storage into geological formations

Jinjin Zhong [1], Xi Jiang [2,*]

[1] Department of Safety Science Engineering & State Key Laboratory of Fire Science, University of Science and Technology of China, Hefei, Anhui 230026, China

[2] Engineering Department, Lancaster University, Lancaster LA1 4YR, United Kingdom

[*] Corresponding author. E-mail: x.jiang@lancaster.ac.uk; Tel: (+44) 1524 592439

Abstract In CO_2 geological sequestration, a combination of monitoring techniques need to be in place to timely detect possible CO_2 leakage from a primary storage along unanticipated pathways to shallower formations. This research aims to methodologically investigate the feasibility of a novel radiographic technique, i.e., cosmic-ray muon radiography, as a complementary continuous monitoring method. As an example, this method was tested on a geological model to monitor CO_2 leakage into upper freshwater aquifers. The effectiveness of the method was preliminarily established by high-fidelity simulations, including the sensitivity for responding to CO_2 leakage and the spatial resolution that can be achieved by the method. The simulation results indicate an increase of penetrating flux of the cosmic-ray muons with the increase of CO_2 leakage in the monitored aquifers. The sensitivity tends to be higher in monitoring leakage taking place in shallower depths. At depths of about 200 m, the detectable CO_2 can be as low as 3% measured in volume fraction with a relatively high confidence level. The spatial resolution can be achieved within a range from 10 m to 20 m for measurements at depths of no more than 520 m, demonstrating the effectiveness of the method.

Keywords CO_2 geological sequestration · Cosmic-ray muons · Feasibility · Leakage monitoring

Introduction

Geological carbon dioxide sequestration in deep underground formations, e.g., subterranean brine formations, depleted oil and gas reservoirs, and coal seams has been studied for more than one decade and is drawing increasing attention with the pressing need for climate change mitigation and greenhouse gas emission reductions, e.g. Anderson and Newell (2004), Hepple and Benson (2004), and Leung et al. (2014). In response to the urgent need of abatement of large amounts of CO_2, it is widely accepted that the best destinations for carbon storage in most cases will be underground formations of sedimentary rock loaded with pores now filled with brine (Socolow 2005). Such storage formations are typically pancake-shaped deposits in the porous subterranean strata, located at least 800 meters deep under low-permeability seals, where the ambient temperature and pressure could maintain CO_2 in a supercritical phase. In the framework of a carbon capture and sequestration project, the long-term effectiveness and safety of the storage reservoir is a major concern after CO_2 injection. Risks must be addressed for every candidate storage reservoir in view of CO_2 migration with time. The CO_2 plume in the storage is buoyant and may lead to leakage to shallower subsurface formations along unanticipated natural geological faults, depleted wells, or through upward seepage due to high pressure and induced fractures, which may in turn pollute potable water resources and defeat the climate goals of carbon sequestration (Nicot 2008; Yamamoto et al. 2009). A combination of monitoring techniques need to be in place for every sequestration project to timely detect possible CO_2 leakage and ensure that impacts on natural resources, such as groundwater and ecosystems, can be mitigated with the shortest possible response time such that the local population will stay unaffected by the leakage (Arts et al. 2004; Park et al. 2013; Wiese et al. 2013).

There are a variety of technologies available for monitoring geological formations, some tried and tested in the oil industry, others as yet unproven (Chadwick et al. 2009). Site monitoring combined with modelling/simulation can play a key role in ensuring storage safety (Jiang 2011; Jiang et al. 2013). Conventional monitoring methods represented by seismic monitoring used in a possible CCS project are episodic. The frequency for these episodic methods is often affected by the storage process, which is higher in the earlier storage period and decreases year by year. Such sites monitoring cannot timely respond to sudden leakage situations that might take place between two measurements. This study aims to further investigate the feasibility of applying a novel radiographic probing method, i.e., cosmic ray muon radiography (e.g. Lesparre et al. 2010; Kudryavtsev et al. 2012), to geological carbon storage site monitoring. The study was motivated by the fact that in the existing studies the simulation processes only considered the variation in the mean density of the monitored volume while the change of constituents was not taken into account. Furthermore, the performance of this method in monitoring CO_2 migration in gaseous state, i.e., CO_2 leakage into shallow formations, has not yet been studied in the literature. In this study, numerical simulations have been performed to detect possible CO_2 leakage from the primary storage into shallower fresh groundwater in the sequestration scenarios in multi-layered formations. With this purpose, this work conducted simulations on a typical geological storage model from Birkholzer et al. (2009), and studied the effectiveness of using time-dependent measurements of the penetrating fluxes of cosmic-ray muons through the monitored volume along different directions as the information source of the internal composition variation caused by CO_2 intrusion and displacement of the in situ groundwater, including its sensitivity to the amount of CO_2 leakage, as well as spatial and temporal resolutions. The optimal zenith angle of cosmic ray muons for monitoring was also analysed, so as to help determine the placement of a muon detector to achieve the best performance.

Traditional radiographic imaging, represented by X-ray scanning of a human body (Mazess et al. 1990), uses the ability of different materials to attenuate the employed ray particles as the imaging property of a targeted object. Generally speaking, the imaging effect of a radiographic method in a specific application depends on the energy spectrum of the radiation source applied in the measurements and the degree of difference of the imaging property of the materials involved in the targeted object (Kak and Slaney 1999; Petersilka et al. 2008). By taking advantage of the highly-penetrating nature of cosmic muons, cosmic-ray muon radiography as a non-destructive probing method has been gaining applications in mapping the inner structure of a geological-scale substance like a mountain (Burkhard et al. 1970; Jenneson 2004; Tanaka et al. 2005). The idea of this method has also been extended to measurements of time-dependent changes occurring within an object. A Japanese team had demonstrated the feasibility of this method to detect both spatial and temporal changes of density inside volcanoes (Nagamine et al. 1995; Tanaka et al. 2009).

In the probing process of this method, cosmic ray muons serve as a naturally occurring radiation source with an inherent time-independent energy and angle distribution. Given a muon detector (Tanaka et al. 2003; Tanaka et al. 2007; Tanaka 2010; Yamashina 2010) with a certain area and exposure duration, the measurement of the integrated penetrating muon fluxes from different directions corresponds to the state of the monitored volume on an average level of the time period. As for the application of CO_2 leakage monitoring, by comparing the subsequent time-dependent measurements after CO_2 injection with the baseline measurement prior to CO_2 sequestration, CO_2 leakage in the monitored volume may be inferred with certain accuracy. The sensitivity of this method in response to CO_2 content determines if the leakage can be interpreted with a high fidelity. This case study performed simulations on various CO_2 leakage levels in different freshwater layers. It is found that this technique has a relatively high resolution in terms of CO_2 volume fraction (which can be easily turned into density fraction) variation in shallow aquifers. The spatial resolution that can be achieved by this method was also studied and assessed, which demonstrates a relatively high fidelity in locating the specific leakage region.

The cosmic-ray muon flux attenuation or penetration behaviour is related to the mean density and material composition along the muon path with zenith and azimuthal angles (θ, Φ) respectively, so detection in one spot can only provide the leakage information in two dimensions. To locate the specific site to which leakage happens, measurements should be made in another spot to cover the potential area and determine the intersection. From the perspective of practical implementations, given the placement of the detectors and their respective angular coverage, the region that is under monitoring could be correspondingly determined. This study mainly concerns with the methodological aspects and the prerequisite problem whether this method can respond to the change in the monitored aquifers caused by CO_2 intrusion and displacement of the in situ pore water within its scanning scope, rather than the construction of a three-dimensional scanning system. The case study in this research shows that cosmic ray muon radiography can be applied as an effective method to perform shallow leakage monitoring. Since this method employs naturally and continuous occurring cosmic-ray muons, it may provide a continuous and cost-effective monitoring way in practical applications. Once leakage was indicated by such continuous monitoring within a certain spatial resolution, other measurements can be further made to obtain more information.

Description of the methods

Cosmic ray muon radiography

Muons are charged particles and share similar properties with electrons except for having about 200 times the mass of electrons. Radiography using the attenuation of muon flux assumes a qualified muon radiation source with a time-independent energy and angle distribution, a well-understood muon detector, and a specific muon propagation model through matter (Schultz 2003; Marteau et al. 2012). The penetration behaviour of the muon flux carries information on the material property along the muon path lines on an average level of the measurement period. Time-dependent changes within the object may be inferred from continuous measurements and analyses. Should variation of matter in either or both material composition and density happen within the scanning scope of the detector, the counting of muon events at corresponding arriving angles would change to a certain number. By comparison between different measurement periods, the material change can thus be inferred and located in two dimensions determined by the muon hitting points on the detector and the recorded directions of the muon path lines through the target object. Three-dimensional determination (Tanaka et al. 2010) of the specific site can be further obtained by one more detection system in another spot in practical implementations.

Cosmic-ray muon source

The earth is continuously bombarded by primary rays from outer space. At an altitude of about 32 km, the primary rays interact with the atmosphere, producing a cascade of secondary particles. By the time this shower of particles reaches the earth surface, it is comprised primarily of muons (Tanaka 2014). Muons are highly penetrating, and among the various possible particles in the secondary radiation, the cosmic muons in high energy region (≥ 100 GeV) are the most suitable for probing into the interior of a geological-scale (≥ 0.1 km) object, as summarized in Table 1 and Fig. 1.

Table 1 Scale of radiography by various particles in the secondary cosmic radiation.

Particle	Basic interactions	Penetration characteristics
Electron, X-ray	Electromagnetic	A few meters or less for conversion
Proton, neutron, pion	Strong and electromagnetic	~ 10 m for absorption
Neutrino	Weak	Earth-size and difficult to detect
Muon	Electromagnetic and weak	100-1000 m and easy to detect

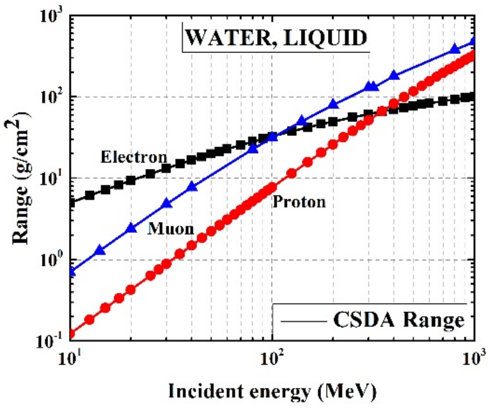

Fig. 1 The mean range of the electron, muon and proton in water and CO_2 (Continuous-slowing-down approximation (CSDA) range, Nakamura and Group (2010)).

Cosmic muons uniformly arrive at every point on the earth surface from angles spanning the upper hemisphere with a wide range of energies. The energy spectrum is azimuthally isotropic, and its dependence on zenith angles has been studied by numerous experiments and theoretical analyses, e.g. Aglietta et al. (1998) and Bugaev et al. (1998). The energy and angle distribution is found to be time-independent, making cosmic muons a quantified radiation source for a radiographic method. The energy distribution of cosmic muons has a wide range from MeV to TeV. As depicted by the model of the modified Gaisser’s formula (Gaisser 1990) in Fig. 2, the muon intensity falls rapidly with energy, and increases with zenith angle in the high-energy region (≥ a few 100 GeV).

The vertical muon rate is about 1 $cm^{-2}\cdot min^{-1}$. The cosmic muons are not applicable for probing objects of small scales, because almost all of the cosmic muons can penetrate through regardless of the material change in the targeted object. While probing large-scale objects, the relatively small intensity in the high-energy region is a potential restricting factor for a specific application, for the reason that an adequate number of muons are needed to be analysed and interpreted in a radiographic scenario while the exposure time period should be restrained in view of the requirement of a temporal resolution as high as possible, especially for measurements of time-dependent changes. Muons arriving from larger zenith angles have a higher intensity, but due to the fact that larger zenith angles mean longer path lengths for muons to penetrate through a geologic body, the probing effectiveness for different zenith angles is to be examined and compared to optimize the placement of the muon detectors.

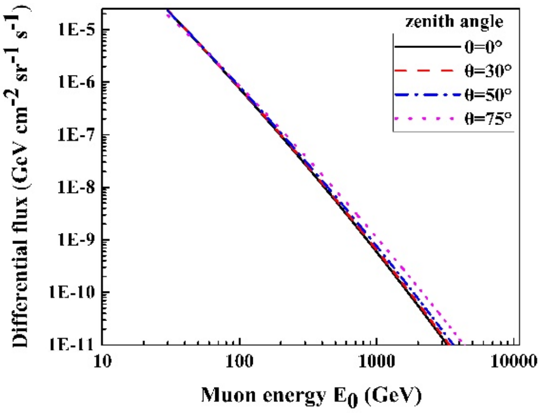

Fig. 2 The energy spectrum of cosmic-ray muons at sea level for arrival angles of near 0°, 30°, 50° and 70° generated from the model of modified Gaisser's formula.

Attenuation of the cosmic-ray muon flux

A detector placed underneath a monitored geological volume is to record the penetrating cosmic-ray muons from different directions. Because the size of a muon detector is much smaller than the object of interest, the direction of each penetrating muon event can be represented by an azimuthal and a zenith angle with reference to a line perpendicular to the detector plane (θ, Φ). The penetrating number N_μ of cosmic muon events as a function of (θ, Φ) in a certain exposure duration is the result of the interactions with matter along the muon paths. A muon flux during propagation in matter will experience two types of changes, which are energy loss and multiple scattering, each leading to muon flux attenuation and defections from their original directions. Muons lose energy through electromagnetic interaction, ionization, and radiative processes, including bremsstrahlung, direct production of e^+ - e^- pairs, and photonuclear interactions (Amsler et al. 2008). The total muon energy loss rate may be summarized as a function of the amount of matter made up of element i traversed by

$$-\langle dE/dx \rangle_i = a(E) + b(E)E \,, \tag{1}$$

where a is the ionization loss and b is the contribution of the three radiation processes (Groom et al. 2001). Both a and b are functions of the muon energy and the material properties Z/A through which muons propagate. In Eq. (1), x is density times length along the muon path ($dx = \rho \cdot ds$, ρ is the density, and ds is the length), representing the amount of matter encountered in unit length.

The mean energy loss rate of a particle in a certain type of material is also referred to as the stopping power of the particle in the material. For a compound or mixture, the mean energy loss rate of the muon is the weighted sum of that for all the elements involved and the weighted fraction for each element is computed by

$$w_j = n_j A_j / \sum_k n_k A_k \, , \tag{2}$$

Then

$$\langle -dE/dx \rangle = \sum_j w_j \, \langle -dE/dx \rangle_j \ . \tag{3}$$

Fig. 3 (left) shows the stopping power for standard rock, water, and CO_2, as a function of muon energy with data from the Particle Data Group (Olive et al. 2015). It can be seen that the stopping power of these three materials differs little from each other, and all of them are slowly varying functions of energy at energies lower than several TeV. The CSDA range mentioned above in Fig. 1 takes an approximation by parameterizing a and b in a continuous-slowing-down way, but it is of limited use, especially for the high-energy region where the stochastic radiative processes have large energy transfer. Taking account of the density of the materials, the mean range of muons of different energy in CO_2 and water is calculated and demonstrated in Fig. 3 (right). It can be seen that the muon with certain incident energy can penetrate a further distance in CO_2 than in water. From another point of view, the critical energy E_c is lower for the muon to penetrate a volume filled with CO_2 than water. Given an incident energy spectrum $\Psi(E, \theta, \Phi)$, the intensity of penetrating muon flux I along the direction (θ_0, Φ_0) can thus be obtained by integrating the energy spectrum from the corresponding critical energy, neglecting the effect of the muon deflections during propagation which will be described subsequently:

$$I\left(\theta_0, \phi_0\right) = \int_{E_c} \psi\left(E, \theta_0, \phi_0\right) \, dE \ . \tag{4}$$

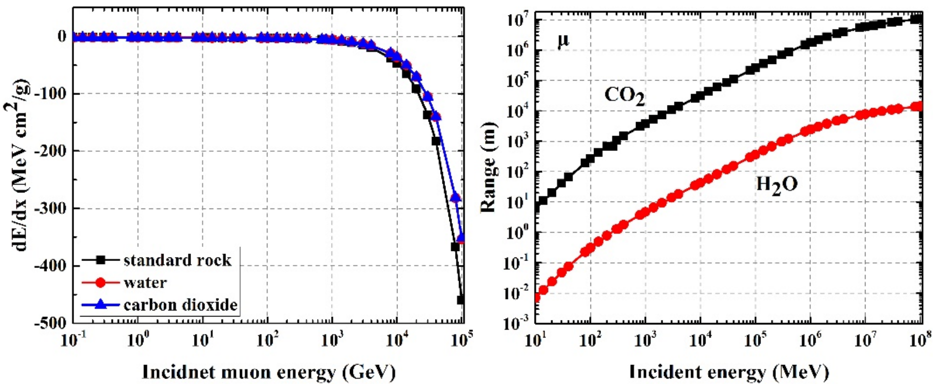

(a) **(b)**

Fig. 3 a The stopping power of the muon in standard rock, water, and CO_2 (with the data taken from pdg.lbl.gov). **b** The muon range (m) in CO_2 and water with different initial energy.

For the application considered in this study, it can be deduced from the above discussion that when CO_2 leaks into the shallower formations of freshwater aquifers and displaces some of the in situ pore water within the scanning scope of the employed detector, more cosmic-ray muons will penetrate through and be detected by the detector placed underneath the monitored volume. The time-dependent measurements could provide information on the change caused by CO_2 leakage and further locate the specific area by measuring from at least two spots.

However, it must be pointed out that the energy loss process has a random nature, and the mean energy loss rate is based on large number statistics rather than an analysis of a single event. Each kind of interaction occurs with their respective cross-sections along the muon path. Detailed energy loss processes require the computation of the cross-sections (i.e., the occurring probability for a type of interaction) (Gaisser 1990) and Monte Carlo modelling of the various interactions (Borozdin et al. 2003) along the muon path. Therefore, the analysis of the penetrating cosmic-muon events should be based on a number large enough for different directions to achieve a relatively high resolution. For practical implementations, the exposure time and the effective area of the employed detector together determine the overall penetrating muon events at one measurement spot. Each parameter should be chosen by considerations of the required temporal resolution and the accessibility of the employed muon detector. The temporal resolution cannot be too long so as to timely respond to CO_2 occupancy, and the size of the detectors should be chosen considering the practical geological conditions to place them.

Muon scattering effect

Besides losing energy during propagation in matter, muons are also stochastically scattered all along the way despite their low cross sections. Every time of scattering slightly influences the muon momentum directions, and multiple scattering processes lead to the muon deflections from their original directions to a certain extent. Accounting for the random nature of scattering, the trajectories of the muons of a certain energy and incident direction are expressed by an angle $\delta\theta$ deflected from the original direction θ, with a probability given by Rayleigh distribution (Priedhorsky et al. 2003):

$$P\left(\delta\theta\right) = \frac{\delta\theta}{\sigma_\theta^2} \exp\left[-\frac{\delta\theta^2}{2\sigma_\theta^2}\right]. \tag{5}$$

The parameter σ_θ, is given by

$$\sigma_\theta = \frac{\alpha}{E}\sqrt{\frac{L}{\xi_0}}\left[1+\kappa \ln\frac{L}{\xi_0}\right]. \tag{6}$$

where α = 13.6 MeV, κ = 0.038, ξ_0 is the radiation length for the traversed material, and L / ξ_0 is the thickness of matter measured by radiation length.

Equations (5) and (6) show that the scattering dispersion largely depends on the muon energy. Since muons lose energy along their paths, the ultimate deflection distribution should be computed along the muon trajectory, taking account of the energy loss. Some approximations can give the mean overall deflection, but they are of limited use, especially for muon propagation through large-scale objects (Lesparre et al. 2010). The detailed processes still need to be simulated by Monte Carlo modelling for each step along the way.

In the process of cosmic ray muon radiography, the penetrating cosmic-ray muons from different directions denoted by (θ, Φ) are deemed to provide the information of the interior of the object along corresponding directions. However, due to the multiple scattering along the muon paths, the penetrating muons from a certain direction may have been deflected from their original direction, which may limit the spatial resolution of this method in a specific application. The muon multiple scattering effect is fully evaluated in the simulation studies to determine the intrinsic spatial resolution of this method in CO_2 leakage monitoring and assess its feasibility in this respect.

Simulation studies

The effectiveness of using cosmic-ray muons attenuation as an information source to detect possible CO_2 gas leakage into freshwater aquifers was investigated by simulations of some leakage scenarios in an idealized multi-layered storage, by considering two aspects of the method, i.e. the intrinsic spatial resolution of this method and its sensitivity for responding to CO_2 leakage.

As an example of application, the simulation studies considered the geological model of the sequestration site from Birkholzer et al. (2009) to examine and assess the applicability of this method. The geometry of the storage is a sequence of 60 m thick aquifers and 100 m thick aquitards extending from the deep saline storage formation to the uppermost freshwater aquifers as depicted in the schematic of the geological structure in Fig. 4. Each layer is assumed to be made up of standard rock and pores filled with brine or freshwater. The material property is obtained from the NIST chemistry book (Lemmon et al. 2010). The porosity is 0.05 in the aquitards and 0.2 in the aquifers respectively, and the hydrogeologic properties are homogeneous in the same layers in the simulation processes. The upper three freshwater aquifers, the 5th, 6th, 7th aquifer (numbered from the bottom storage layer), are the targeted regions to be monitored by placing a muon detector beneath the targeted volumes. Vertical interlayer migration of CO_2 through the sequence of layers into shallow aquifers via local high-permeability conduits such as faults and abandoned boreholes is concerned. The effectiveness of cosmic ray muon radiography on detecting CO_2 leakage into different freshwater aquifers is investigated by numerical simulations using Geant4 (Agostinelli et al. 2003), which is a Monte-Carlo code that could simulate muon propagation in matter with a high accuracy by modelling the interactions between the muon and matter according to their respective cross sections for each step along the muon path. The incident muons were considered to travel from the earth surface down to different depths in the geological model. A muon detector is assumed to be placed underneath the targeted volumes and record the information of the penetrating muons, including their hitting positions, directions and energy. Simulations were carried out corresponding to the baseline measurement prior to CO_2 storage and different leakage scenarios in the storage phase respectively. The information on the penetrating muons are recorded under different geological conditions and analysed to obtain the intrinsic spatial resolution caused by the muon multiple scattering effect and determine the detectable amount of CO_2 by this method.

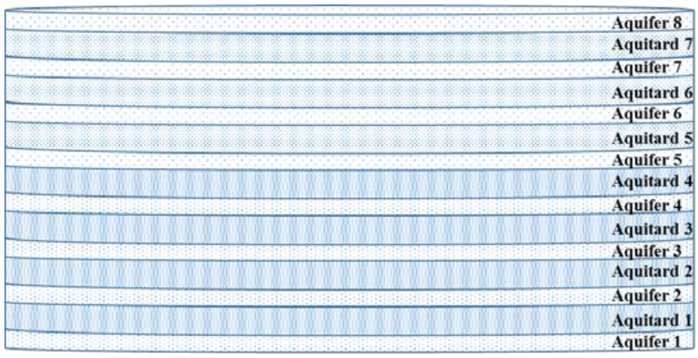

Fig. 4 The schematic diagram of the geological model for the multi-layered storage.

The intrinsic spatial resolution

As discussed previously, the muon scattering effect could impose restriction on the spatial resolution of this method. The muon scattering effect accumulates along the muon paths. The ultimate muon deflection magnitude after traversing a targeted object represents to some extent the intrinsic spatial resolution of this method when applied to probing the object. Therefore, the muon deflections when arriving at the detection panel were studied for several cases to assess the spatial resolution that could be achieved by this method in targeting different depths. This was implemented by starting with considerable amounts of mono-energy muons hitting the earth surface from a single incident point and direction, with these muons propagating through the geological model to different depths subsequently. The scattering processes along the muon paths are stochastic and the deflections under the same condition of the target present a distribution. The dispersion and distributions were analysed and characterized by kernel density estimation in Fig. 5 and Fig. 6.

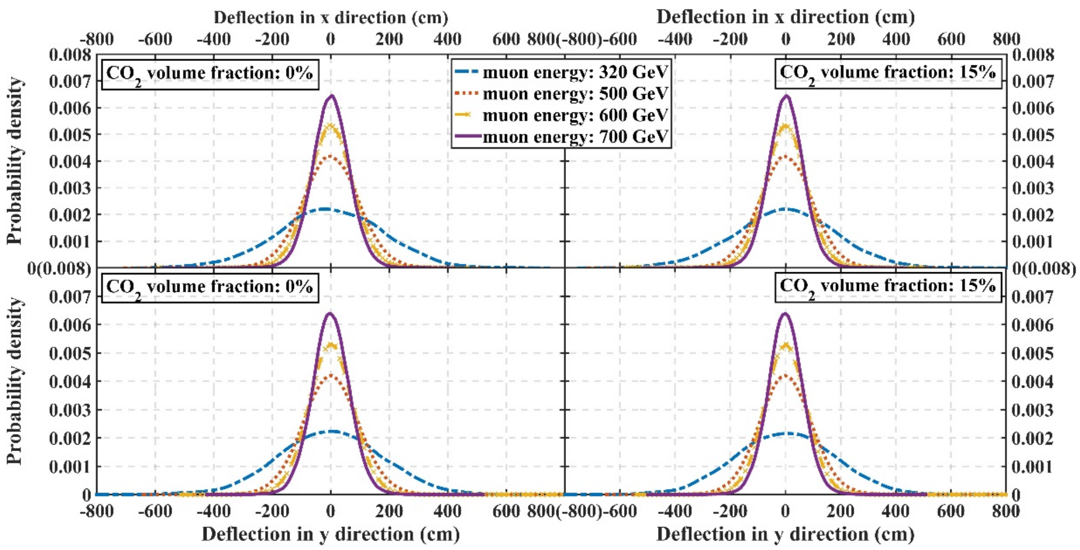

Fig. 5 The deflections of vertically incident muons when arriving at the bottom of the deepest freshwater aquifer (the 5th aquifer) with different incident energies.

The deflections of vertically incident muons at the bottom of the 5th aquifer show that almost all of the muons are distributed within a perimeter of 6 m, which means that the cosmic muons from vertical direction can probe the state of the object above the detector with a spatial resolution at a scale of 10 m. The muon deflections present obvious symmetry in x and y directions because the material is laterally homogeneous which results in azimuthally isotropic distribution. The CO_2 content has a small influence on the deflections, and that is why the scattering effect cannot be the probing property for applications like distinguishing heavy nuclei from others. The extremely-low-probability tails present a small fluctuation in these figures because of the stochastic nature and the small number of such events with large deflections. The distribution becomes narrower with the increase of muon energy, or in other words, the muon flux has a better collimation at higher energies. In light of this result, the largest deflection magnitude can be reasonably studied by the outgoing dispersion of the muons incident with the critical energy to penetrate the whole target, so as to finally determine the spatial resolution. The following simulations were performed on muons with some energy near the critical value for each case to obtain the spatial resolution for the various monitoring cases aiming at different depths.

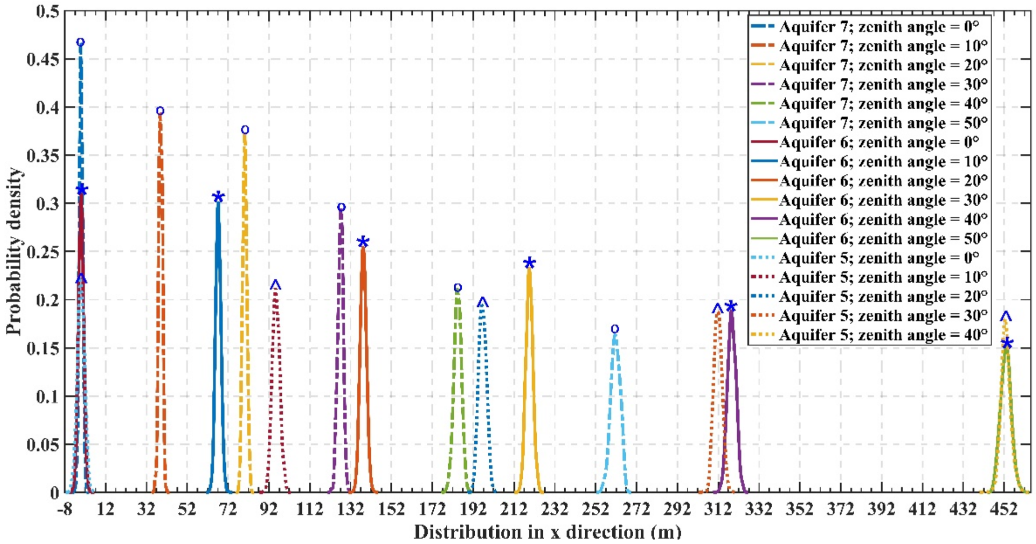

Fig. 6 The largest deflection magnitudes of the muons incident from different zenith angles when arriving at the bottom of the 5th, 6th and 7th aquifers.

Fig. 6 demonstrates the spatial resolutions that can be achieved by the muons from different zenith angles in monitoring the 5th, 6th and 7th aquifers by simulating the largest possible deflection magnitude for different cases. It can be seen that the outgoing spatial distribution tends to be wider with the penetration depth and for the same depth, it grows wider with the increase of the incident zenith angle. This is due to the fact that the increase of either or both the depth and the zenith angle means a longer path for the muons to traverse, and the accumulation of the scattering effect turns more prominent. In summary, the simulation results indicate that this method can achieve a relatively high spatial resolution ranging from 10 m to 20 m. In practical applications, the placement of a detector determines the acceptance range of the zenith angles of the employed cosmic muons and should be optimized by comprehensive considerations of the detection effectiveness of the muons from different zenith angles and the specific requirement of the spatial resolution in an application which will be discussed subsequently.

The sensitivity to CO_2 leakage at different depths

Cosmic ray muon attenuation along different paths through a geological body is supposed to be used as the information soure of the interior variation caused by CO_2 leakage. The sensitivity of this method to detect CO_2 leakage taking place in freshwater aquifers of different depths is investiagted here. For each aquifer to be monitored, a detector was assumed to be placed adjacently beneath it and record the penetrating cosmic muons from different zenith and azimuthal angles, which corresponds to the current state inside the volume above along the muon paths. The simulations for sensitivity study were implemented by changing the CO_2 volume fraction in the aquifers and simulating the penetrating muons for each case by starting with the cosmic-ray muon angular distribution and energy spectrum at sea level with these muons propagating through the geological model to various depths subsequently. The energy spectrum of the cosmic-ray muons at various zenith angles was taken according to the parameterization of Gaisser's formula (1990), modified for large zenith angles with the best fit values for normalization and spectral index obtained by the LVD (large-volume-detector) underground experiment (Robinson et al. 2003).

To determine the detectable amount of CO_2 leakage in the monitored aquifers, the recorded number $N(\theta, \Phi)$ of the penetrating muon events for each leakage case was compared with $N_0(\theta, \Phi)$ for the case without CO_2 leakage and the magnitude of deviation as a response was examined. $N_0(\theta, \Phi)$ represents the baseline measurement prior to CO_2 storage in practice, and $N(\theta, \Phi)$ corresponds to the subsequent measurements after CO_2 injection. It should be noted that in practical monitoring, due to the stochastic nature of the energy loss processes, the measured deviation of N from N_0 not only originates from the change along the path within the targeted volume, but also can be attributed to the intrinsic fluctuations of the penetrating muon number under the same condition of the target volume. When the number of the sampled events is large enough, the distribution of the penetrating number under the same measurement condition can be described in Gaussian function (Young 1962) with the measured value N' at the time as the mean value and $\sigma = \sqrt{N'}$ as the standard deviation. Table 2 indicates the implications of various difference values (denoted by $\Delta = N' - N_0$) between N' and N_0 taking into consideration of the statistical law. To ensure that the confidence level for leakage identification by this method can reach not less than 68%, N' should be out of the region of $N_0 - \sqrt{N_0} \sim N_0 + \sqrt{N_0}$.

Table 2 Confidence level for the variation (Δ) of the penetrating muon events between two separated measurements to be originated from the change within a monitored object.

Δ/σ ($\sigma = \sqrt{N_0}$)	0	0.6745	1	1.6449	2	3
P(Δ)	1.0000	0.5000	0.3173	0.1000	0.0455	0.0027
The confidence level: 1-P(Δ)	0	0.5000	0.6827	0.9000	0.9545	0.9973

Fig. 7 depicts the outgoing number of the cosmic-ray muons after travelling through different targeted volumes (the volumes above the bottom of the 5th, 6th, and 7th aquifer) under various conditions. The symbols represent the outgoing numbers, and the error bars were also drawn by one deviation to highlight the deviation of each leakage case from the baseline case. It has been demonstrated that for penetrating the same path length, a muon needs to have a higher energy level in fresh water than in CO_2 on an average level. As a result, given the energy spectrum at different zenith angles, there would be more penetrating muons from different directions with more CO_2 displacement of water content in a freshwater aquifer. The tendency in these figures shows a coincidence with the qualitative prediction. With the confidence level for CO_2 leakage identification at a relatively high level of 68%, the simulation results show that the sensitivity of this method differs on performing measurements at different depths and with cosmic-ray muons from different zenith angles.

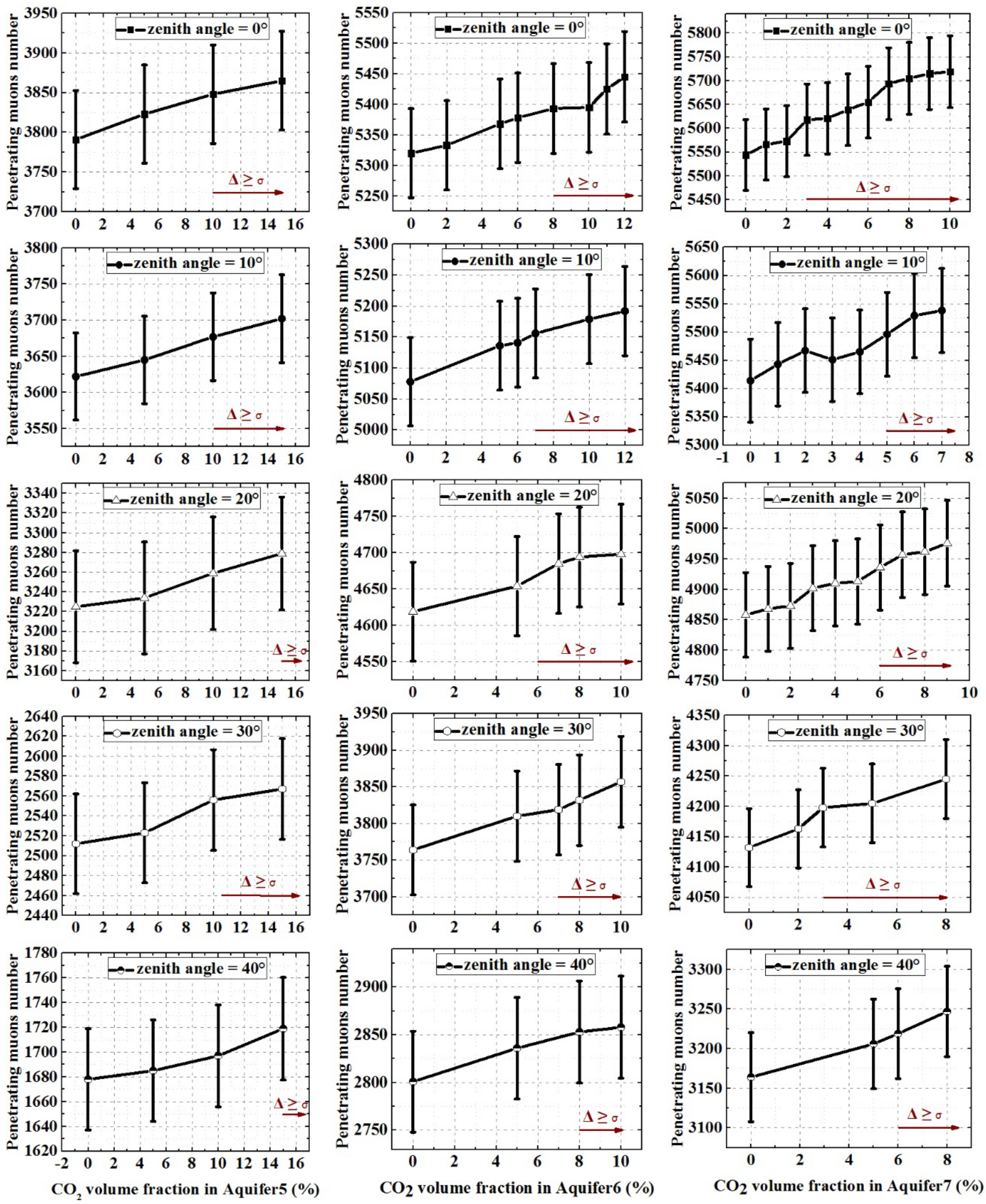

(a) (b) (c)

Fig. 7 The penetrating muons number recorded for baseline case and different cases of CO_2 leakage using a muon detector with a surface area of 1×1 m^2: **a** leakage in the 5th aquifer (measurement period - 23 days); **b** leakage in the 6th aquifer (measurement period - 11 days); **c** leakage in the 7th aquifer (measurement period - 3 days).

To achieve a certain sensitivity, an adequate number of cosmic-ray muons are required to be sampled for one measurement period. By comparing the change in the outgoing muons number in response to various amount of CO_2 leakage in the three sets of figures, this method shows a higher sensitivity in monitoring leakage taking place at shallower depths. That is because the intensity of the cosmic muons decreases as it goes deeper in the underground and with the same exposure duration and detection area, the penetrating muon events that could be sampled are less than at shallower depths. As for leakage in the same depth, muons incident from larger zenith angles will traverse longer path lengths in the leakage region and the amplitude of the change in the mean critical energy for penetration is larger, resulting from that the variation effect in the ability to stop muons before and after CO_2 appearance accumulates more along the way. The ultimate deviation of the penetrating number $N(\theta, \Phi)$ from $N_0(\theta, \Phi)$ is also related to the energy spectrum at that zenith angle. As can be seen from Fig. 7, the best directions to perform with are at about 0° and 10° for the 5th aquifer, 10°, 20° and 30° for the 6th aquifer, and 0°and 30° for monitoring the 7th aquifer.

Fig. 7a shows that with a confidence level of 68%, this method could respond to 10% of CO_2 measured in volume fraction in the aquifer with a temporal resolution of about 23 days using a detector with a sensitive surface area of 1×1 m^2. Fig. 7b shows that should leakage happen in the 6th aquifer, the detectable amount of CO_2 fluctuates between 6% and 8% with a requirement for a longer exposure time period of about 11 days. The sensitivity is highest for detecting leakage in the 7th aquifer as demonstrated in Fig. 7c, and the least possible leakage that can be identified by this method could be as low as 3% of CO_2 within a short exposure duration of about 3 days.

The potential for using the energy of outgoing cosmic muons as an information source

This study goes a step further to explore the potential of using the energy of the outgoing cosmic muons as an information source to identify CO_2 leakage. On an average level, the critical energy for muons to penetrate a monitored area decreases as the amount of CO_2 leakage increases in freshwater aquifers. Taking account of the continuous energy spectrum of the incident cosmic muons, whether this change can be reflected by the statistical information on the energy of the outgoing cosmic muons is yet to be addressed. In order to gain insight into the possibility, the study here considered some CO_2 leakage scenarios taking place in the 7th aquifer as a test. Fig. 8 demonstrates the contrast of the energy distribution and the mean value of the penetrating muons from several zenith angles under different conditions of the 7th aquifer.

The enlarged (zoomed-in) figures in Fig. 8 for the low-energy regions show an identical tendency that due to CO_2 leakage and displacement of the fresh water in the 7th aquifer, the residual energy after penetrating the targeted volume above the detector tends to present a larger proportion in the lower region. The mean energy shows a declining tendency due to the occupancy of CO_2 compared with the baseline measurement prior to CO_2 leakage. This result indicates that the information on the energy of the penetrating muons may serve as another effective source to identify CO_2 leakage, or at least an auxiliary one for identifying the change occurring in the geological formations from the cosmic-muon flux attenuation.

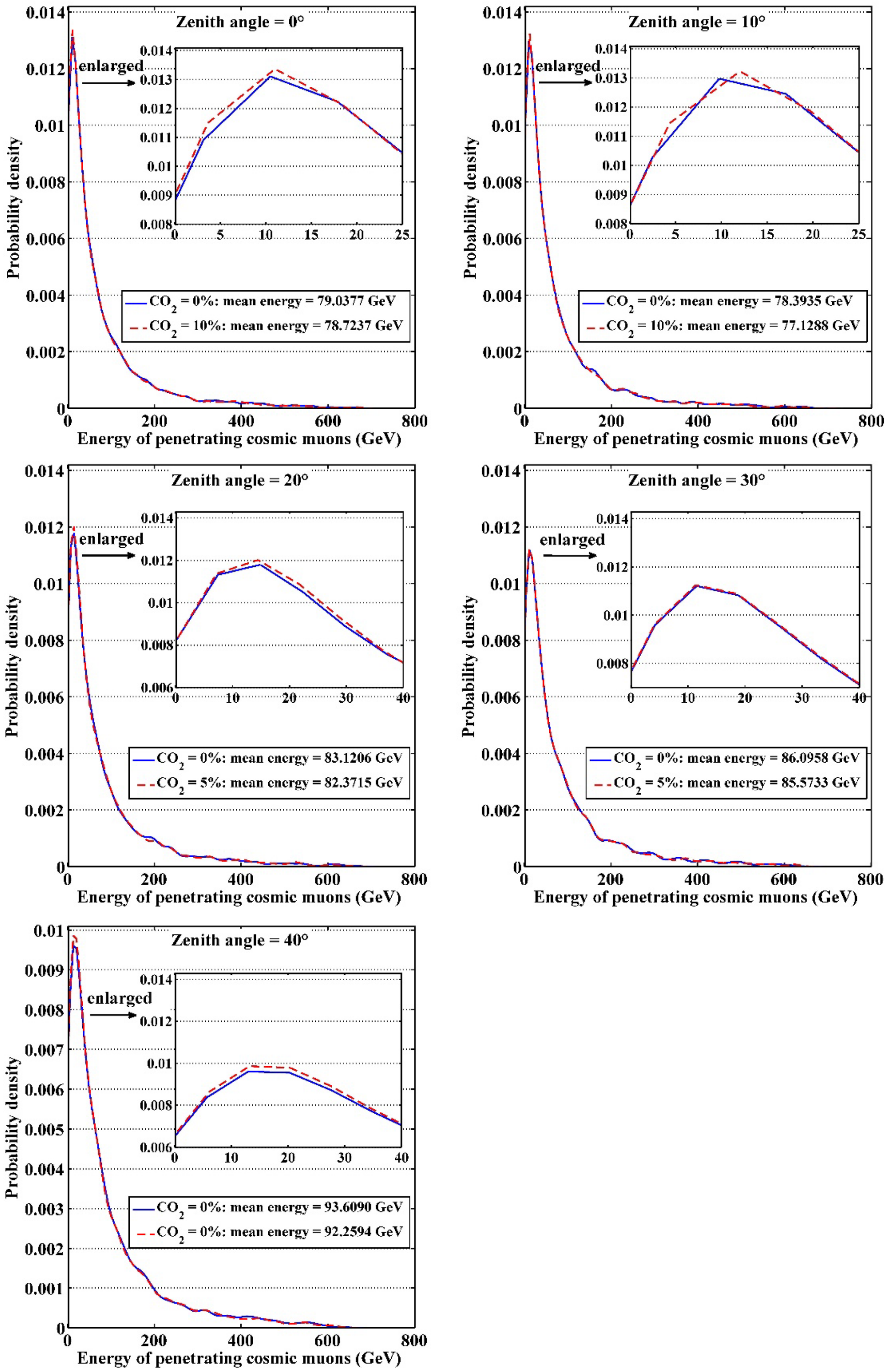

Fig. 8 The energy distribution of the outgoing cosmic muons and their mean energy after penetrating the 7th aquifer under different conditions.

Discussions and conclusions

This study aims to methodologically investigate the feasibility of a novel radiographic method of using cosmic-ray muons attenuation as an information source to monitor possible CO_2

leakage from a primary storage into shallower formations. As an example of application, this method was tested on a multi-layered geological model for CO_2 storage. Its effectiveness in detecting various leakage scenarios in different freshwater aquifers was studied by high-fidelity simulations, including the intrinsic spatial resolution and the sensitivity of the penetrating number in response to the change in the aquifers caused by CO_2 intrusion and displacement.

The spatial resolution of this method is found to be within a range from 10 m to 20 m. Detection at shallower depths tends to have higher spatial resolutions, and for measurements at the same depth, the ability to locate the specific regional leakage is higher for cosmic-ray muons with smaller zenith angles. To achieve a relatively high spatial resolution, the zenith angle of the employed cosmic-ray muons may be chosen not to be larger than 40°. Given a detector with a certain surface area and an exposure period, the sensitivity analysis was performed for using this method to detect possible CO_2 leakage at different depths. It was found that when the volume fraction of CO_2 leakage reaches 10% measured in volume fraction in the shallow freshwater aquifer at depths of about 520 m, it could be identified within a measurement period of 23 days and detection area of 1 m × 1 m. For leakage at shallower depths, the sensitivity tends to be higher, and the detectable amount of CO_2 leakage decreases to as low as 3% with a temporal resolution of two or three days. The thickness for the leakage region is assumed to be 60 m in this study, while the method will be more effective for larger thickness of leakage region under monitoring. The potential for using the energy of outgoing cosmic muons as an information source was also investigated as a preliminary attempt, which demonstrates that it may serve as an effective information source for such monitoring applications or at least an auxiliary one.

To achieve a relatively high sensitivity, an adequate number of cosmic muons is needed. The exposure time and the area of the detector surface can be adjusted and trade-off should be made in consideration of the requirement for the temporal resolution and the geological constraints for the installation of the detection system in a specific practical application. Since the construction of a muon detection system is well-developed nowadays and a detector can be designed and constructed to meet the various requirements for the size and shape, the new monitoring method seems very promising. The radiation source in this radiographic technique is naturally and continuously occurring rather than episodically man-made, making it a cost-effective method for continuous monitoring. The feasibility analysis in this study shows that cosmic-ray muon radiography could serve as an effective complementary way to monitor possible CO_2 leakage into shallower freshwater aquifers. Since it continuously monitors a region of interest, leakage could be identified timely, while other episodic measurements for more information can be taken afterwards.

References

Aglietta, M., B. Alpat, E. Alyea, P. Antonioli, G. Badino, G. Bari, M. Basile, V. Berezinsky, F. Bersani & M. Bertaina (1998) Muon “depth-intensity” relation measured by the LVD underground experiment and cosmic-ray muon spectrum at sea level. Physical Review D, 58, 092005.

Agostinelli, S., J. Allison, K. a. Amako, J. Apostolakis, H. Araujo, P. Arce, M. Asai, D. Axen, S. Banerjee & G. Barrand (2003) GEANT4—a simulation toolkit. Nuclear instruments and methods in physics research section A: Accelerators, Spectrometers, Detectors and

Associated Equipment, 506, 250-303.

Amsler, C., M. Doser, M. Antonelli, D. Asner, K. Babu, H. Baer, H. Band, R. Barnett, E. Bergren & J. Beringer (2008) Review of particle physics. Physics Letters B, 667, 1-6.

Anderson, S. & R. Newell (2004) Prospects for Carbon Capture and Storage Technologies. Annual Review of Environment and Resources, 29, 109-142.

Arts, R., O. Eiken, A. Chadwick, P. Zweigel, L. van der Meer & B. Zinszner (2004) Monitoring of CO_2 injected at Sleipner using time-lapse seismic data. Energy, 29, 1383-1392.

Birkholzer, J., Q. Zhou & C. Tsang (2009) Large-scale impact of CO_2 storage in deep saline aquifers: A sensitivity study on pressure response in stratified systems. International Journal of Greenhouse Gas Control, 3, 181-194.

Borozdin, K. N., G. E. Hogan, C. Morris, W. C. Priedhorsky, A. Saunders, L. J. Schultz & M. E. Teasdale (2003) Surveillance: Radiographic imaging with cosmic-ray muons. Nature, 422, 277-277.

Bugaev, E. V., A. Misaki, V. A. Naumov, T. Sinegovskaya, S. Sinegovsky & N. Takahashi (1998) Atmospheric muon flux at sea level, underground, and underwater. Physical Review D, 58, 054001.

Burkhard, J., A. Fakhry, A. Girgis, A. Goneid, A. H. Moussa & L. Y. Mohammed-Sharkawi (1970) Search for hidden chambers in the pyramids. Science, 167, 832-839.

Chadwick, R.A., R. Arts, M.Bentham, O. Eiken, S. Holloway, G.A. Kirby, J.M. Pearce, J.P. Williamson & P. Zweigel. (2009) Review of monitoring issues and technologies associated with the long-term underground storage of carbon dioxide. In: Evans, D.J. & R.A. Chadwick (eds.) Underground gas storage: worldwide experiences and future development in the UK and Europe. Geological Society, London, Special Publications, 313, 257-275.

Gaisser, T. K. 1990. Cosmic rays and particle physics. Cambridge University Press.

Groom, D. E., N. V. Mokhov & S. I. Striganov (2001) MUON STOPPING POWER AND RANGE TABLES 10 MeV–100 TeV. Atomic Data and Nuclear Data Tables, 78, 183-356.

Hepple, R. P. & S. M. Benson (2004) Geologic storage of carbon dioxide as a climate change mitigation strategy: performance requirements and the implications of surface seepage. Environmental Geology, 47, 576-585.

Jenneson, P. (2004) Large vessel imaging using cosmic-ray muons. Nuclear Instruments and Methods in Physics Research Section A: Accelerators, Spectrometers, Detectors and Associated Equipment, 525, 346-351.

Jiang, X. (2011) A review of physical modelling and numerical simulation of long-term geological storage of CO_2. Applied Energy, 88, 3557-3566.

Jiang, X., W.A. Akber Hassan & J. Gluyas (2013) Modelling and monitoring of geological carbon storage: A perspective on cross-validation. Applied Energy, 112, 784-792.

Kak, A. & M. Slaney 1999. Algorithms for reconstruction with nondiffracting sources. Principles of computerized tomographic imaging. IEEE Press, New York.

Kudryavtsev, V.A., N.C. Spooner, J.G. Gluyas, C. Fung, & M.L. Coleman (2012). Monitoring subsurface CO_2 emplacement and security of storage using muon tomography. International Journal of Greenhouse Gas Control, 11, 21-24.

Lemmon, E., M. McLinden, D. Friend, P. Linstrom, W. Mallard (2010) NIST chemistry webbook, Nist standard reference database number 69. Thermophysical Properties of Fluid Systems, National Institute of Standards and Technology, Gaithersburg.

Lesparre, N., D. Gibert, J. Marteau, Y. Déclais, D. Carbone & E. Galichet (2010) Geophysical muon imaging: feasibility and limits. Geophysical Journal International, 183, 1348-1361.

Leung, D. Y. C., G. Caramanna & M. M. Maroto-Valer (2014) An overview of current status of carbon dioxide capture and storage technologies. Renewable and Sustainable Energy Reviews, 39, 426-443.

Marteau, J., D. Gibert, N. Lesparre, F. Nicollin, P. Noli & F. Giacoppo (2012) Muons tomography applied to geosciences and volcanology. Nuclear Instruments and Methods in Physics Research Section A: Accelerators, Spectrometers, Detectors and Associated Equipment, 695, 23-28.

Mazess, R. B., H. S. Barden, J. P. Bisek & J. Hanson (1990) Dual-energy x-ray absorptiometry for total-body and regional bone-mineral and soft-tissue composition. The American Journal of Clinical Nutrition, 51, 1106-1112.

Nagamine, K., M. Iwasaki, K. Shimomura & K. Ishida (1995) Method of probing inner-structure of geophysical substance with the horizontal cosmic-ray muons and possible application to volcanic eruption prediction. Nuclear Instruments and Methods in Physics Research Section A: Accelerators, Spectrometers, Detectors and Associated Equipment, 356, 585-595.

Nakamura, K. & P. D. Group (2010) Review of particle physics. Journal of Physics G: Nuclear and Particle Physics, 37, 075021.

Nicot, J. P. (2008) Evaluation of large-scale CO_2 storage on fresh-water sections of aquifers: An example from the Texas Gulf Coast Basin. International Journal of Greenhouse Gas Control, 2, 582-593.

Olive, K. A. (2014 and 2015 update) Particle Data Group. Chin. Phys. C, 38, 090001.

Park, Y. C., D. G. Huh & C. H. Park (2013) A Sensitivity Study of Pressure Monitoring to Detect Fluid Leakage from Geological CO_2 Storage Site. Energy Procedia, 37, 4207-4214.

Petersilka, M., H. Bruder, B. Krauss, K. Stierstorfer & T. G. Flohr (2008) Technical principles of dual source CT. European Journal of Radiology, 68, 362-368.

Priedhorsky, W. C., K. N. Borozdin, G. E. Hogan, C. Morris, A. Saunders, L. J. Schultz & M. E. Teasdale (2003) Detection of high-Z objects using multiple scattering of cosmic ray muons. Review of Scientific Instruments, 74, 4294-4297.

Robinson, M., V. Kudryavtsev, R. Lüscher, J. McMillan, P. Lightfoot, N. Spooner, N. Smith & I. Liubarsky (2003) Measurements of muon flux at 1070m vertical depth in the Boulby underground laboratory. Nuclear Instruments and Methods in Physics Research Section A: Accelerators, Spectrometers, Detectors and Associated Equipment, 511, 347-353.

Schultz, L. J. (2003) Cosmic ray muon radiography (Doctoral dissertation). Portland State University.

Socolow, R. H. (2005) Can we bury global warming? Scientific American, 293, 49-55.

Tanaka, H., K. Nagamine, N. Kawamura, S. N. Nakamura, K. Ishida & K. Shimomura (2003) Development of a two-fold segmented detection system for near horizontally cosmic-ray muons to probe the internal structure of a volcano. Nuclear Instruments and

Methods in Physics Research Section A: Accelerators, Spectrometers, Detectors and Associated Equipment, 507, 657-669.

Tanaka, H., K. Nagamine, S. Nakamura & K. Ishida (2005) Radiographic measurements of the internal structure of Mt. West Iwate with near-horizontal cosmic-ray muons and future developments. Nuclear Instruments and Methods in Physics Research Section A: Accelerators, Spectrometers, Detectors and Associated Equipment, 555, 164-172.

Tanaka, H. K. M., T. Nakano, S. Takahashi, J. Yoshida & K. Niwa (2007) Development of an emulsion imaging system for cosmic-ray muon radiography to explore the internal structure of a volcano, Mt. Asama. Nuclear Instruments and Methods in Physics Research Section A: Accelerators, Spectrometers, Detectors and Associated Equipment, 575, 489-497.

Tanaka, H. K., T. Uchida, M. Tanaka, H. Shinohara & H. Taira (2009) Cosmic-ray muon imaging of magma in a conduit: Degassing process of Satsuma-Iwojima Volcano, Japan. Geophysical Research Letters, 36.

Tanaka, H. K., H. Taira, T. Uchida, M. Tanaka, M. Takeo, T. Ohminato, Y. Aoki, R. Nishitama, D. Shoji & H. Tsuiji (2010) Three-dimensional computational axial tomography scan of a volcano with cosmic ray muon radiography. Journal of Geophysical Research: Solid Earth (1978–2012), 115.

Tanaka, H.K.M., T. Uchida, M. Tanaka, H. Shinohara, H. Taira (2010) Development of a portable assembly-type cosmic-ray muon module for measuring the density structure of a column of magma. Earth, Planets and Space, 62, 119-129.

Tanaka, H. K. M. (2014) Particle Geophysics. Annual Review of Earth and Planetary Sciences, 42, 535-549.

Wiese, B., M. Zimmer, M. Nowak, L. Pellizzari & P. Pilz (2013) Well-based hydraulic and geochemical monitoring of the above zone of the CO_2 reservoir at Ketzin, Germany. Environmental Earth Sciences, 70, 3709-3726.

Yamamoto, H., K. Zhang, K. Karasaki, A. Marui, H. Uehara & N. Nishikawa (2009) Numerical investigation concerning the impact of CO_2 geologic storage on regional groundwater flow. International Journal of Greenhouse Gas Control, 3, 586-599.

Yamashina, Y., T. Yamashina, H. Taira, H.K.M. Tanaka (2010) Development of a cost-effective plastic scintillator for cosmic-ray muon radiography of a volcano. Earth, Planets and Space, 62, 173-177.

Young, H. D. (1962) Statistical treatment of experimental data. McGraw-Hill, Inc., New York.